High temperature oxidation of a Cu-Ni based cermet: kinetic and microstructural study

Fabien Rioult, Michèle Pijolat, Françoise Valdivieso, Marie-Agnès Prin-Lamaze

High temperature oxidation of a Cu-Ni – based cermet, Kinetic and microstructural study

Fabien RIOULT[a], Michèle PIJOLAT[a,*], Françoise VALDIVIESO[a], Marie-Agnès PRIN-LAMAZE[b]

[a]*LPMG CNRS UMR 5124, Centre SPIN, Ecole nationale supérieure des mines de Saint-Etienne, 42023 Saint-Etienne, France, mpijolat@emse.fr*
[b]*Alcan CRV, Centr'Alp, BP27, 38340 Voreppe, France, marie-agnes.prin-lamaze@alcan.com*

Abstract

In the course of the development of new materials for inert anodes in the aluminum electrolysis process, cermets have been shown to be good candidates due to combined properties of conduction and resistance to corrosion. At temperatures as high as 900-1000°C, these materials must be particularly resistant, not only to the corrosion by the electrolytic bath, but also to the corrosion by the gaseous atmosphere, which contains oxygen and fluorides. This study was devoted to the kinetics of oxidation in air of a cermet composed with nickel ferrite ($Ni_xFe_{3-x}O_4$), nickel oxide ($Ni_yFe_{1-y}O$) and nickel-copper alloy (Cu_zNi_{1-z}).

First, we present thermogravimetric measurements at 960°C and P_{O2} in the range 1 – 200 hPa and SEM observations of the oxidized samples. The influence of oxygen pressure on the rate of oxidation was determined by means of sudden changes in P_{O2} in the course of oxidation experiments. The data indicate that over a partial oxygen pressure of 51 hPa (P_{Cu}), the oxygen pressure did not influence the rate of oxidation. The presence of the two copper oxides, CuO and Cu_2O explains this independence. Thermodynamically, the coexistence of those two oxides determines the partial oxygen pressure under this interface. Below P_{Cu}, only Cu_2O was detected in the outermost layer of the oxidized samples, and the oxidation rate was found to depend on the oxygen pressure. Complementary analysis by EPMA showed the formation of a sub layer containing a monoxide phase (NiCuFe)O, the consumption of the metallic phases initially present in the bulk of the cermet, with nickel oxide localized around the metal phases. In addition to these modifications, it was observed the dissolution of small amounts of copper inside the grains of nickel ferrite and monoxide.

These results can be explained on the basis of an oxidation mechanism involving both external oxidation (copper oxides formation) and bulk oxidation (nickel oxide formation and reactions between nickel oxide and nickel ferrite). Diffusion of copper towards the surface and diffusion of oxygen inwards the material must account for the rate of weight gain measured in the isothermal experiments, as well as the influence of oxygen pressure in the rage 1 – 51 hPa.

Keywords**:** cermet, oxidation, mechanisms, diffusion, and interfaces.

✓ *Introduction*

Inert electrodes materials have been researched for aluminum production by the electrolysis process, for many years. Currently, the Hall-Heroult process uses carbon anodes that are consumed to react with aluminum oxide and produce evaporating carbon dioxide. This is environmentally and economically disadvantageous for aluminum production industry. Several non-consumable anodes have been tested as copper-nickel-iron alloys [1].

Cermet materials family seems to be good candidates as inert anode materials due to combined properties of conduction and resistance to corrosion. Those materials will have to resist to the electrolytic bath, which temperature approaches 960°C. But it will also have to resist to the corrosion by the gaseous atmosphere that contains oxygen and fluorides. The effect of oxidation by oxygen on a cermet composed of nickel ferrite, nickel oxide and Ni-Cu alloy, at 960°C is studied and presented here. The evolution of the various phases and the effect of oxygen pressure on the oxidation kinetics have been investigated, in order to determine the reaction mechanisms.

First, oxidation kinetics is followed by thermogravimetric measurements in a controlled oxygen pressure atmosphere in the range 1– 1000 hPa, at 960°C. The variations of the rate of oxidation with the oxygen partial pressure were determined by means sudden changes in P_{O2} in the course of oxidation experiments [2].

Then, microstructural evolutions on the material have been studied using SEM observations on several samples oxidized in various conditions. EPMA analysis allowed to follow the composition of the phases.

All the microstructural evolutions can be explained on the basis of an oxidation mechanism. Both external oxidation (copper oxides formation) and bulk oxidation (nickel oxide formation and reactions between nickel oxide and nickel ferrite) have been identified. Oxidation leads to the diffusion of copper towards the surface and the diffusion of oxygen inwards the material.

✓ *Materials and Experimental procedure*

Materials presentation

The material studied to be a possible inert anode is a cermet composed with nickel ferrite ($Ni_xFe_{3-x}O_4$), nickel oxide ($Ni_yFe_{1-y}O$) and nickel-copper alloy (Cu_zNi_{1-z}) (x = 0,8; y = 0,84 and z = 0,56). The weight proportion of each phase, estimated by X-ray diffraction and Rietvelt method, is 44 ± 1 %w for the spinel, 21 ± 2 %w for the monoxide and 35 ± 4 %w for the alloy. Metallic particles (Figure 1, mark a) are spherical with a mean diameter of 20 µm and surrounded and protected by the spinel phase (Figure 1, mark b) that percolates in all the material. The rest is constituted by the monoxide phase (Figure 1, mark c) and porosity (measured to be less than 5% of the volume) (Figure 1, mark d).

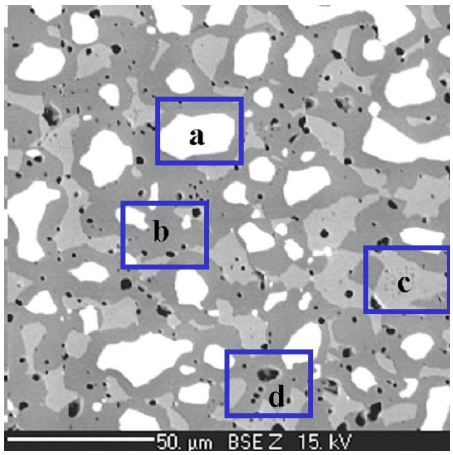

Figure 1: BSE micrograph of non-oxidized Cu-Ni based cermet with (a) Ni-Cu alloy particle, (b) nickel ferrite, (c) monoxide (Ni,Fe)O, (d) porosity.

Sample preparation

The cermet materials were originally delivered in cylindrical bars with a diameter of approximately 15 mm. In order to fit in the thermogravimetric analyzer furnace, we resized it as a 9mm cylinder and sliced 0.5 mm thick disks. This geometry allows to neglect the contribution of the oxidation of the sides of the disks to the weight gain.

Thermogravimetric analysis

Thermogravimetric analyzers (SETARAM TGA24 and TGA92 respectively) were used for all oxidation experiments. The following procedure was applied: the temperature was raised up to 960°C (10°C/min) under flowing argon at atmospheric pressure (10 l/h) in order to prevent the material from oxidation, then at 960°C a flowing mixture of Ar and O_2 is introduced. Flowmeters (BROOKS, 5850E) allowed to control the oxygen partial pressure in the range of 1 – 1000 hPa. At the end of the oxidation experiment in isobaric and isothermal conditions, the temperature was programmed to decrease as fast as the oven permitted (approximately 30°C/min) in order to keep the high temperature microstructure for observations.

During some oxidation experiments, sudden changes in P_{O2} were performed by changing the oxygen and argon flowrate (the total flowrate remaining constant).

Gold markers sputtering

In order to determine if there is an out layer due to the oxidation reaction, gold markers were deposited as drops on the initial surface of a few oxidized samples using BALZERS SCD 050 sputter coater [4]. Gold is chosen as a marker because it is inert in the oxidation conditions of oxygen pressure and temperature.

SEM and EPMA

The SEM observations were performed on a DSM 950 and EPMA analysis on a CAMECA SX100.

All the oxidized samples observed have been prepared with the same process. Cermet disks were cut by half with a diamond disk and coated in a phenolic hot mounting resin with carbon filler. Then they were polished with 180-grains/cm² SiC-papers to 1 micron felt using decane and diamond polishing suspensions respectively. Then samples were cleaned with ethanol.

✓ *Results*

Mass gain curve description

The weight gain versus time of a cermet disk oxidation (Figure 2), at 960°C in 1000 hPa of oxygen, is approximately paralinear. Two different regimes have been identified. A fast mass gain and a rapidly decreasing rate of oxidation correspond to part 1 of the thermogravimetric curve. Then, above 15 g/m², part 2, the rate of oxidation is quasi constant.

Part 1 corresponds probably to the oxidation of the Ni-Cu alloy particles, which are located at the surface of the sample and not protected by the spinel phase. Only part 2 will be described

in this paper, since it represents the long-term behavior of the material, and is the most interesting part for lifetime prediction.

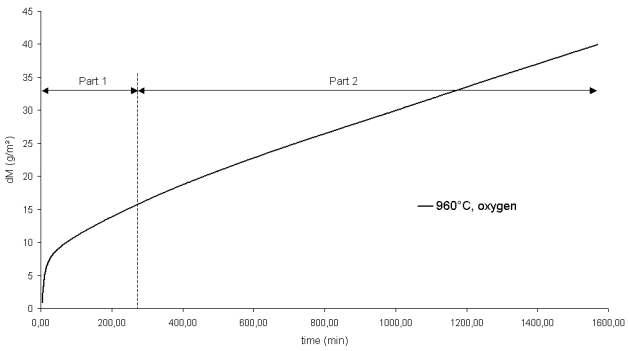

Figure 2: Specific weight gain versus time for 1600 minutes of oxidation at 960°C under 1000 hPa of oxygen.

Influence of the oxygen partial pressure

The influence of oxygen pressure on the rate of oxidation was determined by means of sudden changes in P_{O2} in the course of oxidation experiments (Figure 3, a). A 250 hPa oxygen partial pressure was applied in all the experiments to reach rapidly the part 2 of the mass gain (higher than 15 g/m²) (the higher the oxygen pressure is, the higher the rate of oxidation is in part 1). Then a first sudden change of oxygen partial pressure to 2,5 hPa was performed. After one hour in these conditions the cermet was submitted to a second sudden change of oxygen partial pressure to various values between 2,5 and 250 hPa.

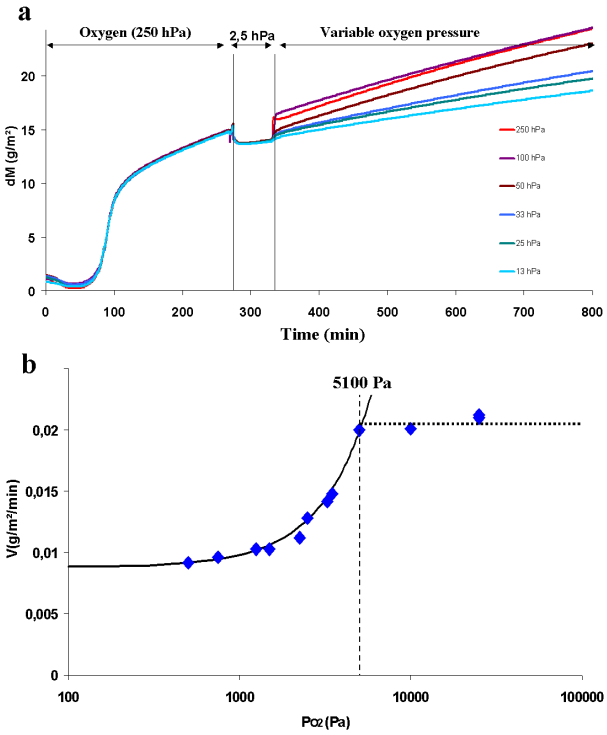

The slope of the mass gain curve, just after the second oxygen pressure change, gives the oxidation rate. The rate of oxidation as a function of the oxygen partial pressure shown in figure 3b, demonstrates that the rate of mass gain increases with the increasing oxygen partial pressure up to 51 hPa. Over this pressure, named P_{Cu}, the rate of oxidation becomes independent of this parameter.

Figure 3: (a) Sudden changes of oxygen partial pressure to variable values between 2,5 and 250 hPa on cermet materials. (b) Rate of oxidation as a function of the oxygen partial pressure.

SEM analysis

Five different characteristic zones, denoted E_1, E_2, P_1, P_2 and C, have been identified during a cermet disk oxidation (Figure 4).

Going from the middle to one surface of the disk, C represents a zone completely similar to the initial material, chemically and morphologically: alloy phases are surrounded by spinel oxide. In Zone P_2, monoxide phases surround the alloy particles and seem to consume the local spinel phase (Figure 5, a and c). On top of this, porosity is created due to the metal phase oxidation. On the contrary, zone P_1 neither contains large pores and copper-nickel alloy particles. Spinel precipitates in the monoxide phases can also be observed in this area (Figure 5, d). Finally, two dense layers have been observed: E_2 and E_1, which are respectively

monoxide and copper oxide phases. The nature of E_1 depends on the oxygen partial pressure. Over 51 hPa, the outward layer is tenorite (CuO) instead of cuprite (Cu_2O) below (figure 6).

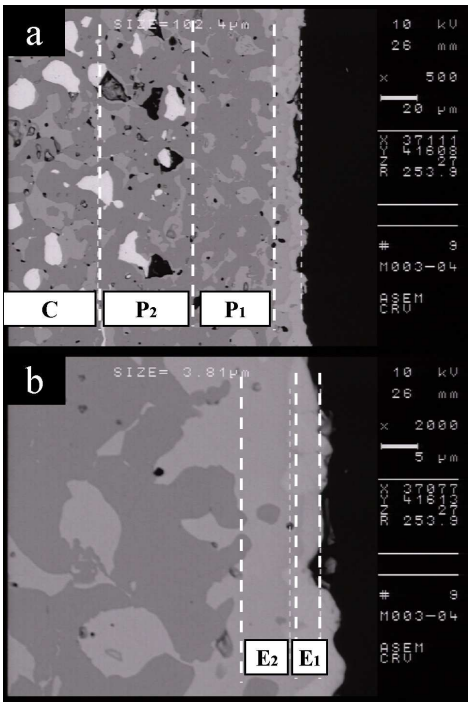

Figure 4: BSE micrograph of a polished cross section of a cermet disk oxidized at 960°C 75 hours in 1000 hPa of oxygen. C, P_1 and P_2 zones are represented on (a). E_1 and E_2 are represented on (b)

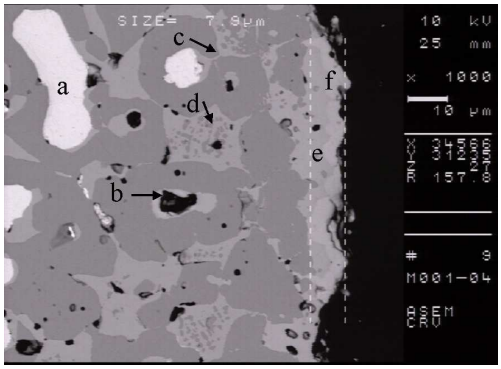

Figure 5: BSE micrograph of a polished cross section of a cermet disk oxidized at 960°C 18 hours in 1000 hPa of oxygen. It shows a Ni-Cu alloy particle surrounded by monoxide (a), porosity formation (b), metal phase surrounded by a monoxide phase that consumes spinel phase (c), monoxide phases that contain ferrite precipitates (d) and a layer of monoxide (e).

Figure 6: BSE micrographs of a polished cross section of cermet disks oxidized at 960°C, 16 hours in 7,0 hPa of oxygen in argon where the outmost layer is Cu_2O (a) and 48 hours in 200 hPa of oxygen in argon where the outmost layer is CuO (b).

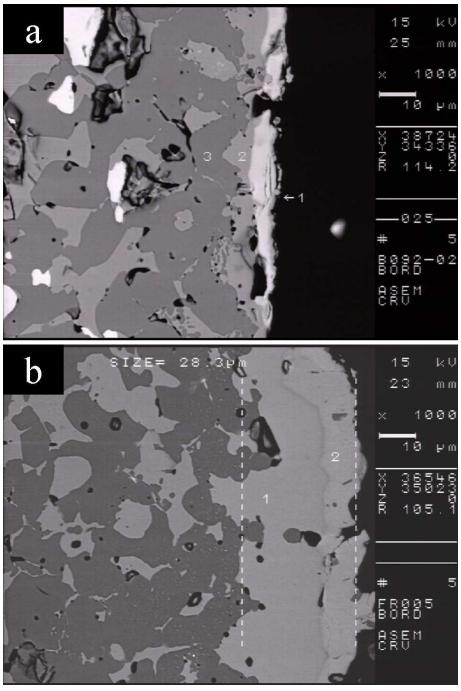

The initial surface can be determined thanks to gold drops deposited on the surface before oxidation (Figure 7). Their localization appears to be the interface between E_2 and P_1, which indicates that E_1 and E_2 are externally grown oxides.

Several samples have been oxidized during different times. The theoretical mass gains due to those external layers have been calculated and compared to the experimental mass gains (from thermogravimetric measurements). It demonstrates that the oxygen content involved in the external oxides is lower than the total reacting oxygen. As external oxidation due to cation diffusion towards the surface does not allow to explain the total mass variation, oxygen diffuses also inwards the material and is responsible for internal oxidation.

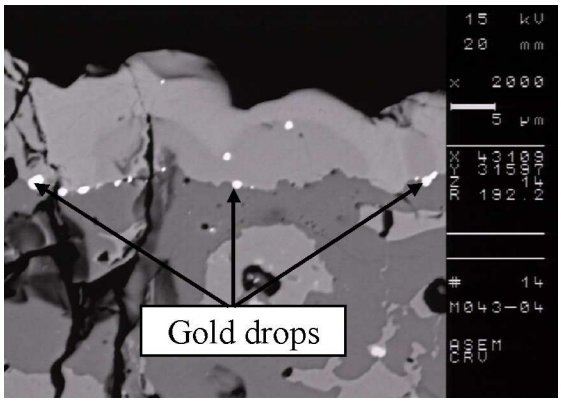

Figure 7: BSE micrographs of a polished cross section of a cermet disk oxidized at 960°C 24 hours in 1000 hPa of oxygen. Gold drops have been deposited by sputtering on the surface of the sample before oxidation.

EPMA analysis

Copper, nickel, iron and oxygen concentrations of a sample oxidized 30 hours at 960°C in 800 hPa of oxygen have been measured, from one side to the other side of the sample, by EPMA analyses. The only cation composing the outmost layer, E_1, is copper and corresponds to CuO in this case (Figure 8). E_2 is the monoxide layer containing all the cations and this phase composition can also be observed in zone P_1. The monoxide contains up to 25%w of copper, which is totally new compared to the initial material. Copper is also detected in the spinel phase of this zone, up to 5%w (Figure 9). On the contrary in P_2, where metal phases subsist, no copper has been detected in the oxides. But the closer the metal phase is to the interface P_1/P_2, the less it contains nickel element (Figure 9).

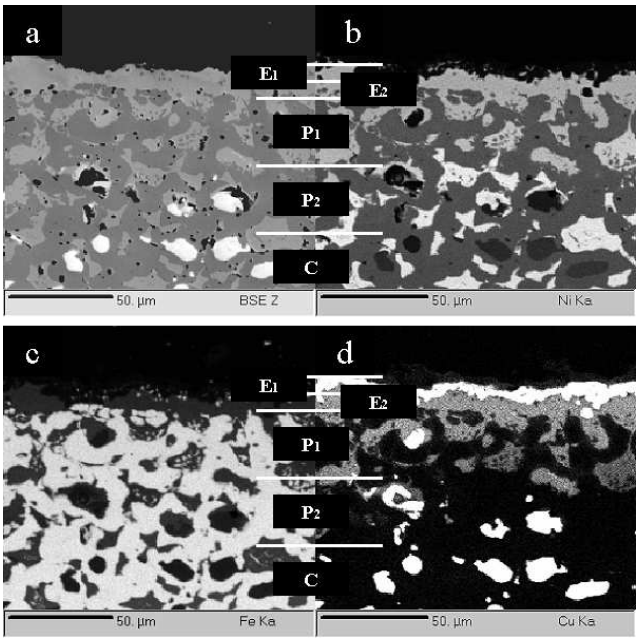

Figure 8: BSE micrograph (a) of a polished cross section of a cermet disk oxidized 30 hours in 800 hPa of oxygen at 960°C and corresponding quantitative EPMA cartography of nickel (b), iron (c) and copper (d).

Considering the spinel phase from C to P_1, the results show that the Fe/Ni ratio decreases and that a small amount of copper enters in the spinel phase. The composition goes from $Ni_{0,8}Fe_{2,2}O_4$ to $Ni_{0,87}Cu_{0,18}Fe_{1,95}O_4$ for the initial and oxidized spinel phase respectively. The Fe/Ni ratio increases in the monoxide phase, and copper insertion in the cubic structure occurs. The chemical composition in zone C is $Ni_{0,84}Fe_{0,16}O$, whereas in P_1 it was measured to be $Ni_{0,59}Cu_{0,29}Fe_{0,12}O$.

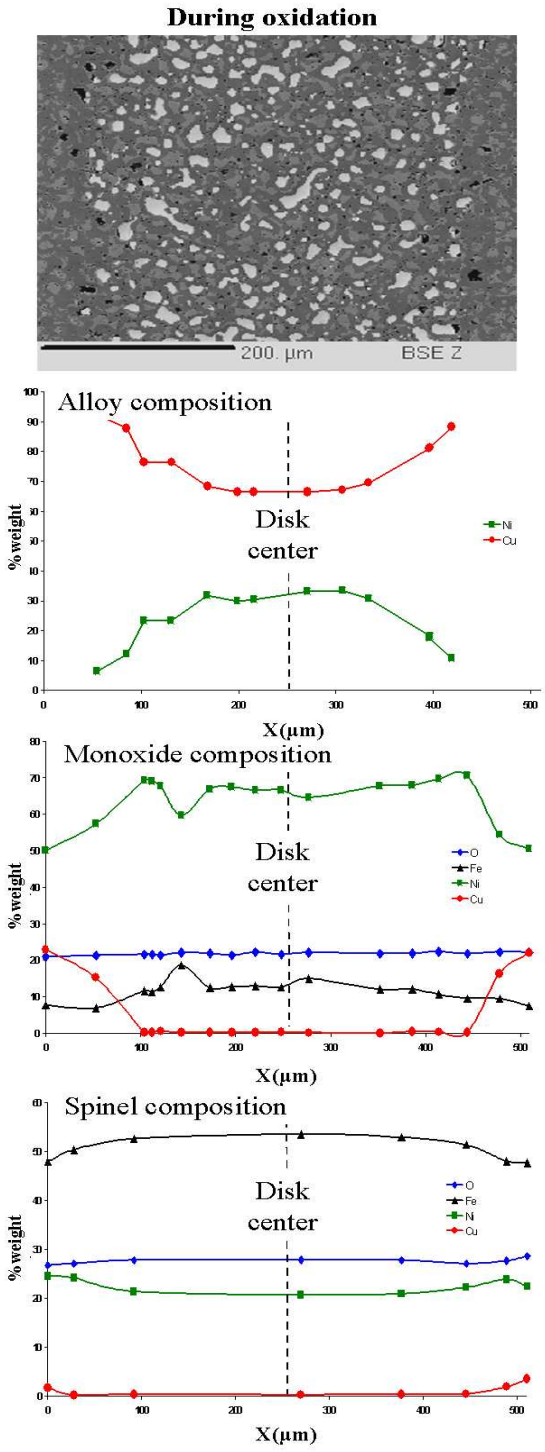

Figure 9:EPMA analysis of a cermet disk oxidized 30 hours in a 800 hPa oxygen – argon atmosphere at 960°C. Nickel, iron, copper and oxygen weight proportion as a function of the position in the disk thickness.

✓ *Discussion*

Kinetics of oxidation

The Oxidation rate increases with oxygen partial pressure up to 51 hPa (P_{Cu}) and becomes independent of this parameter above this value. Microstructural observations demonstrated that this phenomenon was linked with tenorite formation above P_{Cu}. Thermodynamic data [4] confirm that 51 hPa corresponds to the equilibrium oxygen pressure at 960°C between the tenorite and cuprite phases, according to:

$$Cu_2O + \frac{1}{2}O_2 = 2\,CuO \quad (1)$$

Copper oxidation shows the same independence to oxygen partial pressure over P_{Cu} [5, 6]. The coexistence of tenorite over cuprite determines the oxygen partial pressure at this interface. As a consequence, whatever the outside oxygen partial pressure may be, above P_{Cu}, the CuO/Cu_2O interface imposes its equilibrium. Below this pressure, when only cuprite is present at the surface, authors have shown that the copper oxidation rate varies with the oxygen pressure according to: $AP_{O2}^{1/4} + BP_{O2}^{1/7}$. This equation does not fit with our results below P_{Cu}. Thus, diffusion of vacancies through Cu_2O does not control the rate of oxidation on cermet (whereas it is the rate determining step in the oxidation of copper).

All these results lead us to assume that, even if we did not observe the coexistence of the two copper oxides on cermet always oxidized over 51 hPa, the CuO/Cu_2O interface exists. Because the cermet oxidation kinetics is not controlled by the diffusion in Cu_2O, this phase can react rapidly to CuO and the corresponding layer may remain very thin (too thin to be observed).

Microstructural study

Gold markers proved that the oxygen involved in the reaction was partly used for external oxides growth and that the other part diffuses

inwards the material. Only one third of the total reacting oxygen is used for the copper oxide and the monoxide solid solution layers.

EPMA analysis determined that the composition of all the phases changes during the reaction, which means that all the phases of the initial cermet react during the oxidation and interact together. To understand cermet oxidation mechanisms, it will be necessary to take into account all the interfaces and possible cation exchanges between alloy, monoxide and spinel.

Nickel oxide and copper oxides are known to contain cation vacancies. Spinel phases as nickel ferrite and iron oxide can contain, both, cation vacancies and interstitial cations [7, 8, 9, 10, 11, 12, 13, 14]. Those common properties of the different phases, containing major cationic defects, explain easily the external oxides growth but not the diffusion of oxygen inward the material. As a consequence, considering oxidation reaction via volume diffusion would only allow an external growth of oxides [15]. Then the mass gained during the oxidation should correspond to the oxygen contained in the external oxide layers. This contradiction with the experiments leads us to think that grain boundary diffusion might take place in the cermet. Consequently, the cermet oxidation mechanism will have to take into account a cation flux towards the surface and an inwards oxygen flux.

Knowing the phases that appear, their localization, and the evolution of their chemical composition, it is possible to propose mechanisms of oxidation of the cermet material.

Oxygen adsorption on the material surface is the first reaction to occur during the oxidation. First, oxygen will react rapidly with the alloy particles on the surface of the disk directly in contact with the gas, which represent part 1 of the mass gain curve. Considering part 2 of the oxidation, copper oxide already exists on surface. The oxygen can either contribute to the growth of copper oxide or diffuse inwards the material via grain boundaries. If copper oxide is formed, a cation vacancy will result in the tenorite, or cuprite, layer and will diffuse also inwards.

We will describe first the consequence of direct inward diffusion of cation vacancies. Then, in a second part, we will consider the grain boundary oxygen diffusion.

A cation vacancy (V_c) diffusing inwards the material through P_1 can first react with the monoxide to create spinel precipitates. This means that the vacancy replaces a cation (Me) migrating outwards. 4 cations plus 4 oxygen ions become 3 cations plus 4 oxygen ions, which corresponds to the spinel formation according to equation (2).

$$V_c + 4\,MeO \rightarrow Me_c + Me_3O_4 \qquad (2)$$

It implies that iron included in monoxide oxidizes to Fe (III) to create spinel phases from monoxide in zone P_1. It corresponds exactly to the mechanism of internal oxidation of monoxides via cation vacancies described by Schmalzried [16].

But iron oxidation is a small part of the cermet oxidation weight gain compared to nickel and copper oxidation. Consequently, a minor quantity of the available vacancies can be used for reaction (2). Then, a majority of the vacancies will diffuse through P_1 to react with the alloy particles in zone P_2. Reaction of those defects at the Spinel/alloy interface first consumes the nickel present in the alloy and then copper. The nickel reacts with the vacancies and the oxygen contained in the spinel phase to form a monoxide surrounding the alloy particle

(Figure 4, zone P_2). Vacancies coming from the surface, it explains that the monoxide observed around the metal is localized preferentially on the side of alloy particles that are closer to the surface of the sample. Then, once the alloy becomes copper-rich, copper begins to react with the vacancies to diffuse towards the surface. Thus, the formation of the monoxide phase accounts for nickel consumption from the metal phase in zone P_2 and the spinel consumption. It explains the interface advance of C/P_2 inwards the material.

Only one third of the weight gain corresponds to the cation vacancies diffusion from the surface. Oxygen diffusion through grain boundaries is responsible of the two other thirds. The low porosity in zone P_1 is certainly due to the reaction of these oxygen species with the material. The pores issued from the metal migration make it possible for oxygen to react with the surface of the pore and create monoxide. New cation vacancies are produced by this reaction and will diffuse inwards the material in zone P_2. Then, those cation vacancies will follow the reactions described previously for the cation vacancies coming from the sample surface reaction: creation of spinel precipitates in monoxide (equation 2) or oxidation of metallic nickel and copper. This mechanism allows to understand the porosity disappearance in zone P_1 and the advance inwards the sample of the interface P_1/P_2.

✓ *Conclusions*

The cermet oxidation can be divided in two parts. Part 1 is certainly due to the fast oxidation of the alloy particles at the surface of the samples. The rate of oxidation decreases rapidly to become quasi constant in part 2. The long-term behavior of the material is represented by the second part of the oxidation. During this part, two oxide layers, copper oxide and monoxide (Ni,Cu,Fe)O, are formed on the outer scale. Cuprite and tenorite, depending on the partial oxygen pressure, constitute the outmost oxide. Two other characteristic zones have been identified. Zone P_1, which contains few porosity and no metal particles, and zone P_2 where the nickel of the alloy reacts with the oxygen of the spinel phase to form a monoxide surrounding the alloy. Copper migrates towards the surface and creates porosity in zone P_2.

The oxidation reaction rate increases with oxygen pressure below 51 hPa. Over this pressure value (P_{Cu}), coexistence of cuprite and tenorite imposes its equilibrium, which explains the oxygen partial pressure independence of oxidation kinetics over P_{Cu}.

The two oxide layers are externally grown phases. This has been demonstrated using gold markers to localize the initial surface on an oxidized sample. Oxygen involved in those layers only represents one third of the total weight gain during the reaction. Consequently, the two other thirds of oxygen must diffuse inwards the materials.

The inner oxidation is certainly the result of grain boundary oxygen diffusion in the material, and oxide formation in the porosity. Whatever the oxidation way is, nickel contained in the alloy is the first element to oxidize, creating a monoxide phase surrounding the alloy phase. Then copper migrates towards the surface and is oxidized in monoxide, spinel and copper oxide. Spinel precipitates apparition in monoxide is the result of iron oxidation but its contribution to the weight gain can be neglected.

References

1. R. Haugsrud, T. Norby, P. Kofstad, "On the high temperature oxidation of Cu-30wt%Ni-15wt%Fe", *Corrosion Science*, **43**, 283-299 (2001).
2. M. Tupin, M. Pijolat, F. Valdivieso, M. Soustelle, A. Frichet, P. Barberis, "Kinetic study of the oxidation by oxygen of a zirconium based alloy: ZrNbO, Difference between the pre- and post-transition stages", *J. Nuclear Materials*, **317**, 130-144 (2003).
3. P. Sarrazin, A. Galerie, J. Fouletier, "Les mécanismes de la corrosion sèche", *edited by EDP Science*, 68-69 (2000).
4. FactSage System, 2004, www.factsage.com
5. R. Haugsrud, P. Kofstad, "On the oxygen pressure dependence of high temperature oxidation of copper", *Material Science Forum*, **251-254**, 65-72 (1997).
6. R. Haugsrud, P. Kofstad, "On the high temperature oxidation of Cu-rich Cu-Ni alloys", Oxidation of metals, *edited by Springer Science*, **50**, 189-213 (1998).
7. K. Tsukimura, S. Sasaki, N. Kimizuka, "Cation distributions in nickel ferrites", *Jpn. J. Appl. Phys.*, **36**, 3609-3612 (1997).
8. W. Chul Kim, S. Jin Kim, S. Wha Lee, S. Hee Ji, "Atomic migration and superexchange interaction in $Ni_{0,1}Cu_{0,9}Fe_2O_4$", *IEEE transactions on magnetics*, **36**, 3399-3401 (2000).
9. M. N. Khan, A. Memon, S. Al-Dallal, "Structural, electrical and spectroscopic studies of the system $Ni_{1-x}Cu_xFe_2O_4$", *Int. J. Electronics*, **76**, 953-959 (1994).
10. F.Haab, Th.Burhmester, M. Martin, "High temperature in situ X-ray absorption studies on the iron valence in iron doped nickel oxide $(Ni_{1-x}Fe_x)_{1-\Phi}O$", *Solid State Ionics*, **141-142**, 289-293 (2001).
11. W.C. Tripp, N.M. Tallan, "Gravimetric determination of defect concentration in NiO", *J. Am. Ceram. Soc.*, **53**, 531-533 (1970).
12. F.A. Kröger, "The chemistry of imperfect crystals", *edited by North-Holland Publishing Company*, 406-418 (1964).
13. N. L. Peterson, W.K. Chen, D. Wolf, "Correlation and isotope effects for cation diffusion in magnetite", *J. Phys. Chem. Solids*, **41**, 709-719 (1980).
14. S.H. Kang, H.I. Yoo, "Nonstoechiometry and high-temperature thermodynamic properties of $(Mg_{0,22}Mn_{0,07}Fe_{0,71})_{3-d}$ ferrite spinel", *J. of Solid State Chemistry*, **145**, 276-282 (1999).
15. P. Kofstad, "High temperature corrosion", *edited by Elsevier applied science*, London and New York, 162-240 (1988).
16. H. Schmalzried, "Chemical kinetics of solids", *edited by VCH*, Weinheim, 211-217 (1995).